Synthetic Aperture Radar Pulse Compression with Optimized Nonlinear Frequency Modulation

Asmaa O. Helmy[1, 2], Ashraf S. Seliem Mohra[1], and Khalid F. A. Hussein[3, *]

Abstract—The present paper proposes a novel technique to reduce the peak side lobe ratio (PSLR) in the time waveform of the synthetic aperture radar (SAR) pulse. The dependence of the instantaneous frequency on the time over the SAR pulse duration is formulated as an arbitrarily shaped piecewise linear (PWL) curve. The slopes of the linear segments of this curve are optimized to get the minimum PSLR of the received radar echo at the output of the SAR receiver. The particle swarm optimization (PSO) method is used to optimize the shape of the time-frequency curve to achieve the dual-objective of minimizing the PSLR of the received SAR echo and to realize the required pulse compression ratio (PCR). The slopes of the linear segments of the time-frequency curve are the control parameters that determine the position of each particle in the swarm. The proposed method can be considered as an optimized form of nonlinear frequency modulation (NLFM) for SAR pulse compression. It is known that the conventional NLFM using second-order time-frequency curve results in a PSLR of -18 dB. The proposed method results in a PSLR of -45.6 dB and achieves a range resolution of 1.4 m. The developed PSO algorithm is shown to be computationally efficient, and its iterations are fastly convergent such that a few iterations are enough to arrive at the steady state of the cost function. Finally, a SAR transceiver is proposed as a software-defined radio (SDR) in which the proposed SAR pulse compression technique is employed in the transmitter to generate the transmitted pulse and in the receiver to construct the transfer function of the matched filter (MF).

1. INTRODUCTION

Synthetic Aperture Radar (SAR) is the most important system for earth remote sensing irrespective of the land-imaging time and the varying whether conditions [1–4]. High resolution and enhanced performance of SAR target detection are the most important requirements for satisfactory SAR systems [5]. A narrow SAR pulse is necessary for high imaging resolution. On the other hand, a pulse of long time duration is required for enhanced radar performance by increasing the pulse energy and, hence, the signal-to-noise ratio (SNR) without increasing the peak power [5]. Thus, a trade-off between the imaging resolution and detection performance always exists. SAR pulse compression is employed to enhance the imaging resolution of the land-imaging SAR system without the need to increase the transmitted power [6]. In SAR pulse compression schemes, the SAR pulse is formed to have longer time duration for enhancing the imaging performance regarding the SNR, and in the meantime, it has a wide frequency band to simulate a shorter pulse for enhancing the imaging resolution (see Figure 1). The most common technique of SAR pulse compression is the pulse chirping by applying linear frequency modulation (LFM).

A great deal of the recent research work in the field of SAR system design has focused on the SAR transceiver design as a software-defined radio (SDR) [7–13]. In SAR receivers employing pulse
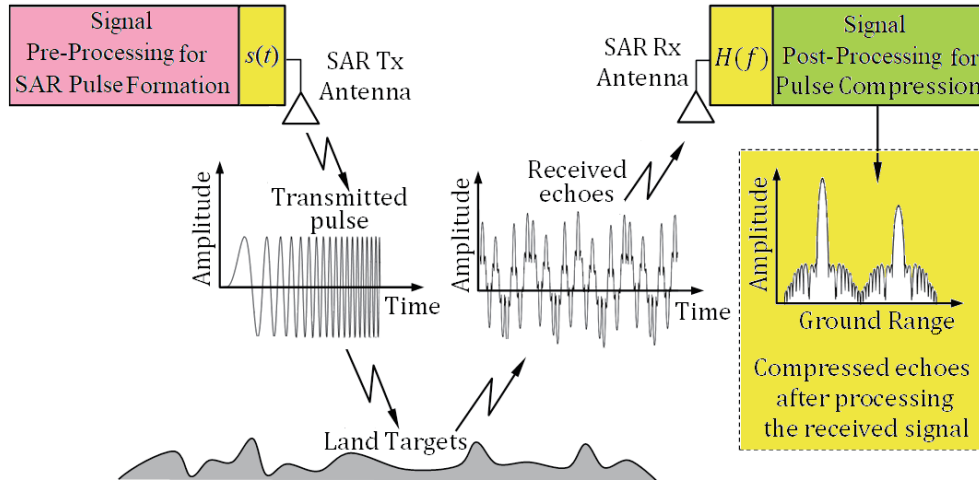
Figure 1. Compression of the transmitted pulse for improving the SAR resolution [13] and enhancing the detection performance.

compression schemes as mentioned above, the received echo is processed through a matched filter (MF) to get the received SAR echo at the MF output in the form of a pulse with a main lobe and multiple side lobes of much lower level. One of the other benefits of the MF of the SAR system receiver is to maximize the SNR, thereby improving the receiver sensitivity and enhancing the SAR detection performance. Also, the MF improves the imaging resolution by suppressing the side lobes of the received SAR echo after processing. The MF response to the LFM chirped pulse achieves a peak side lobe ratio (PSLR) of about -13 dB. Many techniques have been proposed to improve the PSLR produced by the LFM such as time and frequency windowing, adaptive filtering [14], and many optimization methods [15]. Such techniques are able to improve the PSLR relative to that produced by the conventional LFM but usually result in reducing the SNR and a wider main lobe (i.e., a lower pulse compression ratio) than those achieved by the conventional LFM. Also, nonlinear frequency modulation (NLFM) is commonly employed in SAR systems to produce high imaging resolution and acceptable SNR.

A lot of recent publications have been concerned with introducing new compression schemes of the SAR pulse for enhancing the detection performance and SAR resolution. For example, in [16], the starring spotlight mode is proposed for high resolution imaging SAR with low PSLR. The NLFM is employed for low PSLR in the range direction, whereas the azimuth nonuniform sampling (ANUS) is employed for low PSLR in the azimuth direction. Owing to the application of this method, a compressed SAR pulse with PSLR of -22 dB is produced. In [17], piecewise NLFM waveforms are proposed to produce compressed SAR pulse with low PSLR. These waveforms are composed of three subcarriers of different types and mathematical formulations. The application of this method achieves PSLR of -27 dB. The work of [18] proposes a method that employs orthogonal frequency-division multiplexing (OFDM) waveform to produces PSLR of -28 dB. The work of [19] proposes a piecewise NLFM technique to obtain a compressed SAR pulse whose time waveform has three segments. The first and third segments are LFM waveforms, whereas the second segment is an NLFM waveform. A PSLR of -36.6 dB is realized when this method is applied to compress the SAR pulse. The scheme proposed in [20] is based on the optimization using Lagrangian method and results in PSLR of -38 dB. In [20], advanced NLFM waveform is applied to obtain PSLR of -40 dB. In [22], a method based on NLFM optimized by genetic algorithm is introduced and gives PSLR of -40.6 dB.

The present paper proposes a novel technique to reduce the PSLR of the radar pulse for enhanced detection performance and high resolution of the SAR system. The dependence of the instantaneous frequency on the time over the transmitted pulse duration is formed as an arbitrarily-shaped piecewise linear (PWL) curve. The slopes of the linear segments of this curve are optimized using the particle swarm optimization (PSO) [23] to optimize the time-frequency curve for achieving the dual optimization goals of minimizing the PSLR and realizing the desired pulse compression ratio (PCR). A

computationally efficient PSO algorithm is developed for this purpose. The slopes of the linear segments of the time-frequency curve are the control parameters that determine the position of each particle in the swarm. The proposed method can be considered as an optimized NLFM for SAR pulse compression. The developed PSO algorithm is shown to be computationally efficient, and its iterations are perfectly convergent such that a few iterations are enough to arrive at the steady state of the cost function. The proposed SAR pulse compression technique is employed to implement software-defined transmitter and receiver (transceiver) of the SAR system.

The next section of the present paper explains the frequency modulation for chirping the SAR pulse. Section 3 explains the proposed scheme for SAR pulse processing in the transmitter and receiver. Section 4 describes the application of the PSO to construct the optimized shape of the time-frequency curve for frequency modulation of the SAR pulse. Section 5 provides clear presentations with important discussions of the numerical results. Finally, Section 6 highlights the conclusions of the present paper.

2. SAR PULSE COMPRESSION BY FREQUENCY MODULATION

One of the most commonly used methods for radar pulse compression is the pulse frequency chirping using second-order relation between the instantaneous frequency and the time. The SAR pulse has the time waveform of a sinusoidal signal with increasing frequency over the pulse duration.

2.1. Time Waveform of the NLFM Chirped SAR Pulse using Second-Order Dependence of the Frequency on the Time

Over the duration of the SAR pulse, the transmitted signal can be expressed as follows:

$$s(t) = \sin \theta_i(t) \tag{1}$$

where $\theta_i(t)$ is the angle from which the instantaneous frequency, $f_i(t)$, which can be obtained as follows.

$$f_i(t) = \frac{1}{2\pi} \frac{\partial \theta_i(t)}{\partial t} \tag{2}$$

For quadratic (second-order) NLFM for chirping the SAR pulse the instantaneous frequency, $f_i(t)$ takes the following expression.

$$f_i(t) = A(t - T_B)^2 + \frac{B - AT^2}{T}(t - T_B) + f_B, \qquad T_B \leq t \leq T_E \tag{3}$$

where T_B and T_E are the start and end times of the pulse; B is the bandwidth; T is the pulse duration; and A is a constant. The center frequency, $f_C = (f_B + f_E)/2$, is the operating frequency of the SAR, where f_B and f_E are, respectively, the start and stop frequencies and can be expressed as follows.

$$f_B = f_C - \frac{B}{2}, \qquad f_E = f_C + \frac{B}{2} \tag{4}$$

The angle $\theta_i(t)$ can be obtained by integrating the instantaneous frequency with the time to get,

$$\theta_i(t) = 2\pi \left[\frac{A}{3}(t - T_B)^3 + \frac{B - AT^2}{2T}(t - T_B)^2 + f_B(t - T_B) + C \right], \qquad T_B \leq t \leq T_E \tag{5}$$

where C is a constant of integration equal to $\theta_i(t = T_B)$, i.e., the angle at the start time of the SAR pulse.

Setting $C = 0$ in (5) results in zero-phase of the sinusoidal waveform at the start of the pulse. In this case, $\theta_i(t)$ can be expressed as follows.

$$\theta_i(t) = \frac{2\pi A}{3}(t - T_B)^3 + \frac{\pi(B - AT^2)}{T}(t - T_B)^2 + 2\pi f_B(t - T_B), \qquad T_B \leq t \leq T_E \tag{6}$$

2.2. Sampling Process (Time and Frequency Discretization)

In the present work, the performance assessment of the proposed pulse compression scheme is performed through realistic simulation. The pulse formation, transmission, reception, and processing chain are simulated through a computer program developed using Matlab®. For this purpose, the time and frequency are discretized to apply the operations of the fast Fourier transform (FFT) and its inverse (IFFT). The start time of the nth sampling period is

$$t_n = (n-1)\,\delta t + T_B, \qquad T_B = (n_B - 1)\,\delta t, \quad n = 1, 2, \ldots, N \tag{7a}$$

where N is the number of time samples of the transmitted SAR pulse, $s(t)$. Let the time interval between the successive samples be δt. n_B is the index of the time sample at which the transmitted pulse starts. The total time for simulation is $T_T = L\delta t$, where L is the total number of sampling periods over which the simulation is performed. The nth frequency component of the discrete Fourier transform of the transmitted pulse can be expressed as,

$$f_n = f_B + (n-1)\,\delta f, \qquad \delta f = \frac{1}{L\delta t}, \quad n = 1, 2, \ldots, N \tag{7b}$$

The sampling frequency, $f_S = 1/\delta t$, should satisfy the condition $f_S \geq 2f_E$ for accurate results of the simulation.

3. PROPOSED SAR SYSTEM RECEIVER BASED ON PWL FREQUENCY MODULATION

In this section, the proposed preprocessing algorithms required for SAR pulse formation in the transmitter and for the construction of the MF of the receiver are described. Also, the design of SDR transceiver based on this method is introduced.

3.1. Preprocessing for SAR Pulse Formation and Construction of MF Transfer Function

In the present work, an optimized PWL time-frequency curve is proposed as a method of NLFM for SAR pulse compression. The proposed digital pre-processing is presented in Figure 2. The transmitted SAR pulse, $s(t)$, is constructed in the transmitter by the aid of the PSO algorithm where the instantaneous frequency is transferred to a voltage signal to be the input of a software-defined voltage controlled oscillator (VCO), which, in turn, generates a sinusoidal signal whose frequency is proportional to the input voltage. The output of the VCO is multiplied by the output of a pulse envelop generator that is responsible for determining the pulse repetition rate (PRR), pulse duration, and pulse amplitude. The time-frequency curve, $f_i(t)$, is stored in the transmitter memory with the appropriate sampling rate. On the other hand, the FFT operation is applied to the chirped SAR pulse, $s(t)$, to get its spectrum, $S(f)$. The transfer function, $H(f)$ of the MF is then calculated as the conjugate of $S(f)$.

$$H(f) = S^*(f) \tag{8}$$

The frequency samples of $H(f)$ are separated by δf that is determined by the FFT as $\delta f = (L\,\delta t)^{-1}$ as described in Subsection 2.2 and given by (7). The frequency samples of $H(f)$ (both magnitude and phase) are stored in the memory of the SAR receiver.

The inputs to the PSO algorithm are the pulse design parameters which are the SAR pulse width, T, the number of linear segments, Q, of the time-frequency curve, and the weights required to formulate the cost function. The latter is constructed as the summation of two terms; the first term is the calculated PSLR multiplied by a weighting factor W_{SLL}, and the second term is the difference between the achieved PCR and the desired PCR, which is multiplied by the weighting factor W_{PCR}. The developed PSO algorithm and its application for constructing the time-frequency curve is explained, in detail, in Section 4.
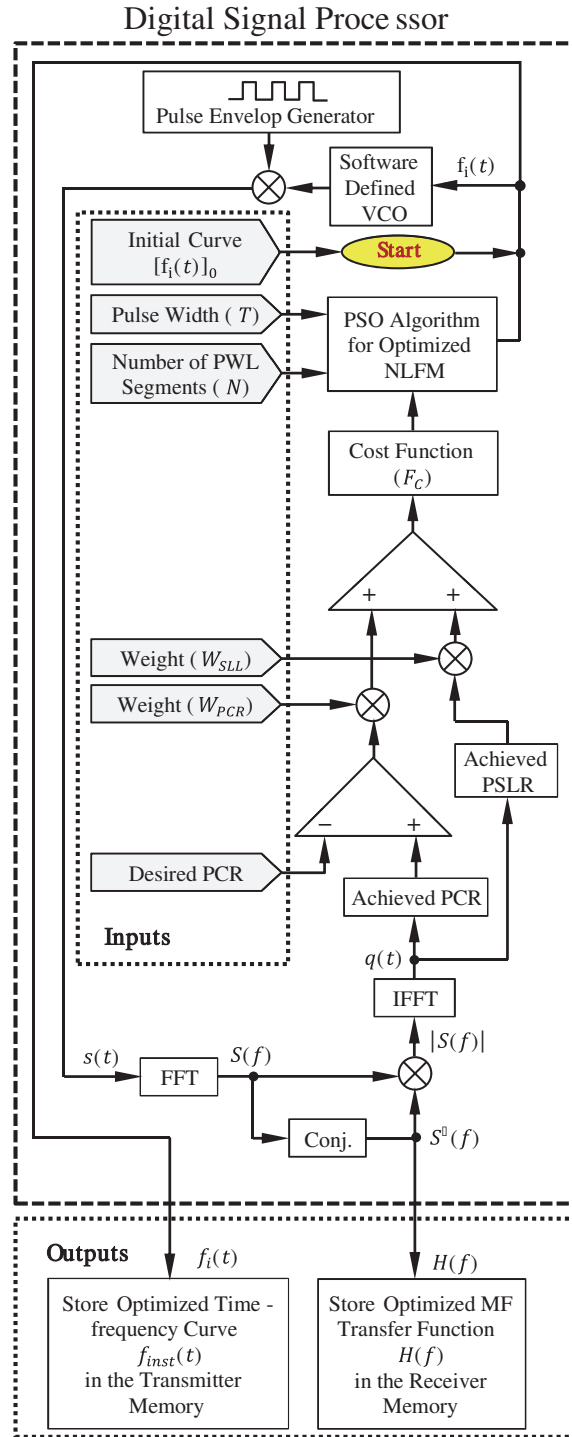
Figure 2. Block diagram of the proposed digital signal processing algorithm for the proposed software defined SAR transceiver.

3.2. Proposed SAR System Transceiver

A transceiver based on the preprocessing method described in Subsection 3.1 can be constructed. The block diagrams of the SDR transmitter and receiver are presented in Figures 3 and 4, respectively. The SDR transmitter has its all operations implemented as software modules except for the fast digital-to-
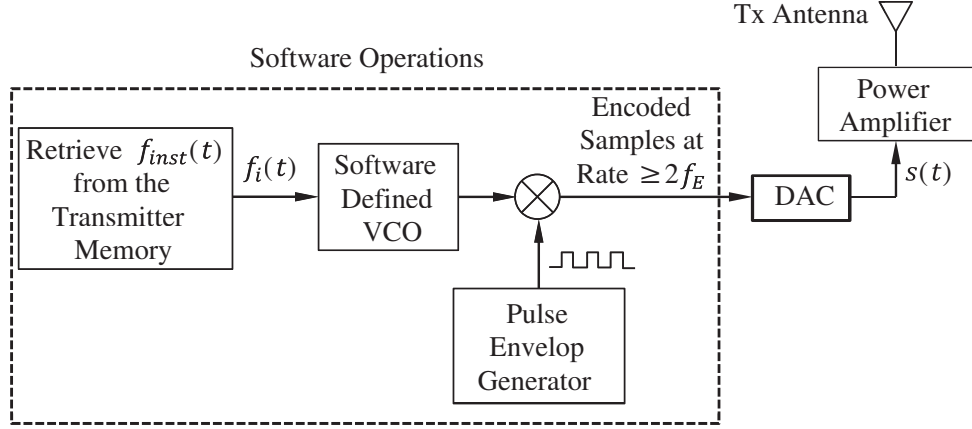
Figure 3. The proposed SDR transmitter of the high resolution SAR system.
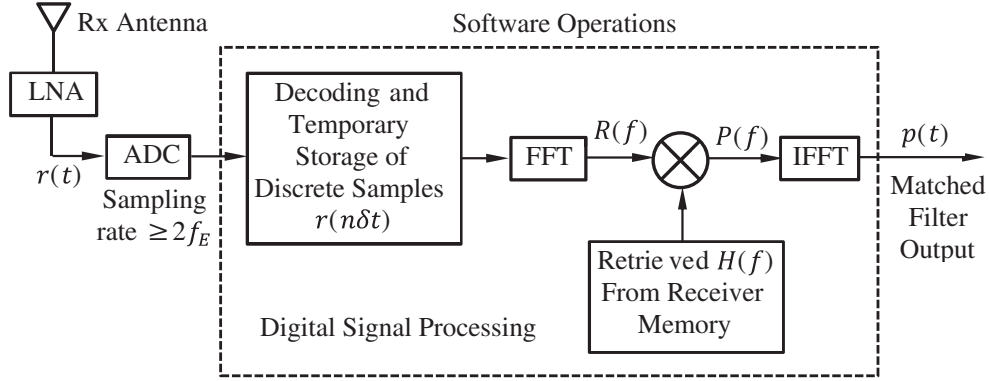

Figure 4. Block diagram of the SDR receiver proposed for high resolution SAR system.

analog converter (DAC) and the following power amplifier (PA) shown in Figure 3. In the transmitter, the optimized time-frequency curve, $f_i(t)$, that has been constructed in the preprocessing stage described in Subsection 3.1 is retrieved from the transmitter memory. The instantaneous frequency is transformed to a voltage signal to be the input of a software-defined VCO, which, in turn, generates a sinusoidal signal whose frequency is proportional to the input voltage. The transmitted SAR pulse, $s(t)$, is constructed in the transmitter by multiplying the output of the VCO by the output of a pulse envelop generator that is responsible for determining the pulse repetition rate (PRR), pulse duration, and pulse amplitude.

The MF of the SAR receiver has its transfer function, $H(f)$ given by (8) as the conjugate of the transmitted signal. This function is constructed and stored in the receiver memory using the preprocessing algorithm explained in Subsection 3.1 and illustrated in the block diagram shown in Figure 2. The block diagram of the proposed SDR receiver of the SAR is presented in Figure 4. This receiver has its all operations implemented as software modules. Only the low-noise amplifier (LNA) and the fast analog-to-digital converter (ADC) are implemented as hardware modules. The spectrum of the processed SAR echo at the MF output can be expressed as follows,

$$P(f) = H(f) R(f) \tag{9}$$

It can be assumed that the received echo $r(t)$ is the same as the transmitted signal, $s(t)$, but with modified magnitude and phase due to scattering on the SAR target. Thus, the following expression can be written for the spectrum of $r(t)$

$$R(f) = A_0 e^{j\varphi_0} S(f) \tag{10}$$

where A_0 and φ_0 are the magnitude and phase modifications due to scattering of the SAR pulse upon

incidence on the land target. Thus, the spectrum, $P(f)$, of the received echo can be expressed as follows

$$P(f) = |S(f)|^2 A_0 e^{j\varphi_0} \tag{11}$$

In the SDR receiver, the processed SAR echo, $p(t)$, is obtained by applying the IFFT to $P(f)$. From (11), it is shown that the frequency band of the processed SAR echo, $p(t)$, is the same as that of the transmitted pulse, $s(t)$.

4. OPTIMIZED TIME-FREQUENCY CURVE FOR HIGH RESOLUTION AND ENHANCED PERFORMANCE

The method of optimization of the time-frequency curve proposed to minimize the PSLR of the signal at the output of the SAR receiver and to satisfy a desired value of the PCR is described in detail in this section. Initially, the dependence of the instantaneous frequency on the time is formulated as an arbitrarily shaped curve close to that of a quadratic equation with PWL segments, and then the a computationally efficient PSO algorithm is applied to satisfy the optimization goals by arriving at the optimum time-frequency curve.

4.1. Proposed Scheme for Nonlinear Frequency Modulation

The proposed PWL segmentation of the instantaneous frequency as a function of time produces a type of NLFM for SAR pulse compression with varying sweep rates. Let Q be the number of linear segments constructing the nonlinear curve of the instantaneous frequency as a function of time and Δt be the duration of each linear segment as shown in Figure 5. Thus, the start and end times of the qth linear segment are t_{q-1} and t_q, respectively. The rate of frequency sweep of the qth linear segment is s_q.
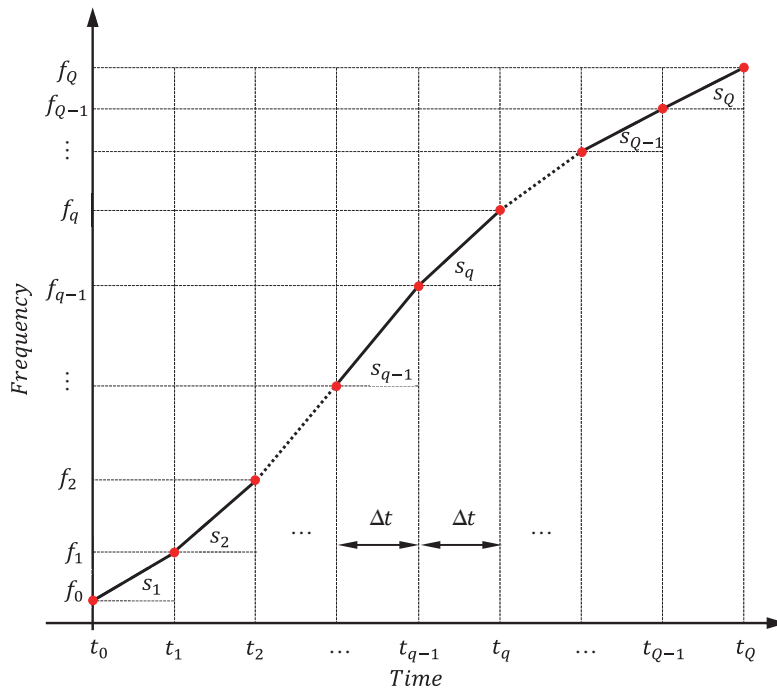

Figure 5. The dependence of the instantaneous frequency on the time is constructed as PWL curve.

The time duration of the SAR pulse can be given as follows,

$$T = t_Q - t_0 = Q\Delta t \tag{12}$$

where,

$$t_0 = T_B \tag{13}$$

The slope of the qth linear segment of the time-frequency curve can be given as,

$$s_q = \frac{f_q - f_{q-1}}{t_q - t_{q-1}} = \frac{f_q - f_{q-1}}{\Delta t} \tag{14}$$

Thus, the qth frequency component of the chirped SAR pulse can take the following expression

$$f_q = f_{q-1} + s_q \Delta t \tag{15}$$

The PWL curve that describes the instantaneous frequency f_i as a function of the time is presented in Figure 5. This relation should be continuous, i.e., the successive linear segments of the curve should be connected. However, the slopes $\{s_1, s_2, \ldots, s_Q\}$ can be varied so as to minimize the PSLR for a specific (desired) PCR. The PSO method is applied to optimize the shape of the curve describing the dependence of the instantaneous frequency on the time. This is achieved by selecting the best values of the slopes $\{s_1, s_2, \ldots, s_Q\}$ to realize the optimization goals. The PSO algorithm developed for this purpose is described in detail in Subsection 4.2. The number of segments of the time-frequency curve, Q, has a great effect on the optimization results. This is explained and discussed in Section 5 where the numerical results are presented.

4.2. Application of PSO to Construct the Optimized SAR Pulse

The developed PSO aims to construct time-frequency curve considering that the slopes of the continuously linked linear segments of this curve are the control parameters that determine the position of each particle in the swarm. It is required to arrive at the optimum values of the slopes of the linked linear segments to satisfy the optimization goals. The optimization goals are to achieve the required PCR with the minimum PSLR of the processed echo signal at the output of the SAR receiver.

4.2.1. Optimization Problem

In the optimization problem described above, the position of each particle of the swarm is determined by a set of the slopes $\{s_1, s_2, \ldots, s_Q\}$. The swarm has 15 particles where the initial position of each particle is set to realize a second-order dependence of the instantaneous frequency on the time with little random perturbations to get the initial curves representing the positions of the particles different from each other.

The PSO algorithm aims to iteratively reduce the cost function that is formulated as follows.

$$\mathcal{F}_{cost} = W_{SLL}\ell + W_T |T_A - T_D| \tag{16a}$$

where ℓ is the achieved PSLR, T_A the achieved pulse duration, T_D the desired pulse duration, W_{SLL} the weight factor of the PSLR, and W_T the weight factor of the deviation of the achieved pulse width from the desired pulse width. Alternatively, the cost function can be constructed as described by the block diagram of the digital signal preprocessing shown in Figure 2 to get the following expression.

$$\mathcal{F}_{cost} = W_{SLL}\ell + W_{PCR} |C_A - C_D| \tag{16b}$$

where C_A is the achieved PCR, C_D the desired PCR, and W_{PCR} the weight factor of the deviation of the achieved PCR from the desired one.

The developed PSO algorithm runs iteratively to calculate the optimum slopes of the PWL segments constructing the time-frequency curve. In each iteration, the particle position is determined by the Q-dimensional vector given by the set of slopes $\{s_1, s_2, \ldots, s_Q\}$. The process described by the block diagram shown in Figure 2 is applied to get the shape of the processed SAR echo, $p(t)$ at the receiver output. However, for constructing the chirped transmitted pulse, the optimization process needs a feedback from the received pulse, $p(t)$. As this pulse has not yet obtained, a simulated version of $p(t)$ is obtained in the transmission by including an MF in the transmitter, which is identical to that of the receiver. The simulated version of $p(t)$ is $q(t)$. From this simulated version, the achieved PSLR and PCR pulse can be calculated to provide the inputs required for the PSO algorithm as shown in Figure 2.

4.2.2. Implementation of the PSO Algorithm

In the process of PSO, the swarm of particles advances progressively towards the optimization goal. Each particle position is, actually, a solution of the main problem. During the swarm motion, each particle changes its velocity making advantage of its past position and also the information gained from the other particles. The particles change their positions according to the new velocity. Thus, in the progressive iterations of the PSO algorithm, each particle position is a solution that has a cost value evaluated by the cost function that is formulated to be reduced while approaching the optimization goals. The best solution of the main problem, i.e., the particle that has the best position within the swarm results in the lowest value of the cost function. Each particle records its individual best position; also, it records the global best particle position in the swarm. Accordingly, each particle changes its velocity considering its best position and the best particle position in the swarm. The PSO algorithm has two tactics, called global tactics and local tactics. In the global tactics, each particle tracks the position of the best particle of the swarm. In the local tactics, each particle tracks its own optimal position. The overall tactics is that the particle tracks its own best position, and in the same time it tracks the position of the best particle in the swarm.

After initializing all the particles positions, $\mathbf{x}_\nu^{(0)}$, and velocities, $\mathbf{v}_\nu^{(0)}$, the PSO algorithm starts its progressive iterations. Each iteration can be divided into four sequential stages: (i) evaluation of the local best position $\mathbf{y}_\nu^{(\tau)}$, for each particle, (ii) evaluation of the global best particle position, $\mathbf{g}$, among all the particles positions, (iii) evaluation of the new velocity, $\mathbf{v}_\nu^{(\tau+1)}$, of each particle, and finally, (iv) evaluation of the new position $\mathbf{x}_\nu^{(\tau+1)}$ of each particle. Then the PSO algorithm advances to the next iteration to execute the four stages. The PSO algorithm stops when the cost function remains unchanged over a number of iterations.

In the optimization problem of the present case, the position vector of the νth particle is the vector whose components are the slopes of the PWL time-frequency curve, i.e.,

$$\mathbf{x}_\nu^{(\tau)} = \left(s_1^{(\nu,\tau)}, s_2^{(\nu,\tau)}, \ldots, s_q^{(\nu,\tau)}, \ldots, s_Q^{(\nu,\tau)} \right)^{Trans} \tag{17}$$

where superscript "$Trans$" means the transpose of the array.

The velocity and position of the νth particle in the τth iteration of an iterative PSO algorithm are, respectively, calculated as follows

$$\mathbf{v}_\nu^{(\tau)} = u\mathbf{v}_\nu^{(\tau-1)} + c_1 r_1 \left[\mathbf{y}_\nu^{(\tau-1)} - \mathbf{x}_\nu^{(\tau-1)} \right] + c_2 r_2 \left[\mathbf{g}^{(\tau-1)} - \mathbf{x}_\nu^{(\tau-1)} \right] \tag{18}$$

$$\mathbf{x}_\nu^{(\tau)} = \mathbf{x}_\nu^{(\tau-1)} + \mathbf{v}_\nu^{(\tau)} \tag{19}$$

where τ is the index of iteration; u is the coefficient (weight) of inertia; c_1, c_2 are the cognitive and social rate coefficients; and r_1, r_2 are randomly generated numbers in the range 0–1.

During the iterations of the PSO algorithm the velocity $\mathbf{v}_\nu^{(\tau)}$ is not allowed to exceed maximum limit, and the following constraint should be applied.

$$\left| \mathbf{v}_\nu^{(\tau)} \right| \leq V_{\max} \tag{20}$$

If the magnitude of the velocity $\mathbf{v}_\nu^{(\tau)}$ for one of the particles exceeds $V_{\max}$, it is forced to be equal to $V_{\max}$.

4.2.2.1 Initialization of the Particles Positions

The position of each particle can be initialized by assigning a set of initial values to the slopes $s_1^{(\nu,0)}$, $s_2^{(\nu,0)}$, ..., $s_q^{(\nu,0)}$, ..., $s_Q^{(\nu,0)}$, and these initial values can be determined by initializing the time-frequency curve corresponding to each particle as a second-order dependence of the frequency on the time, as described in Subsection 2.1 with small random perturbations as shown in Figure 6. The second-order time-frequency curve is described by (3) where parameter A is set to the value that results in the best performance of a second-order NLFM pulse chirping regarding the PSLR. The optimum value of A can be obtained to realize that the instantaneous frequency is as close as possible to $f_c = 1.27\,\text{GHz}$ at the
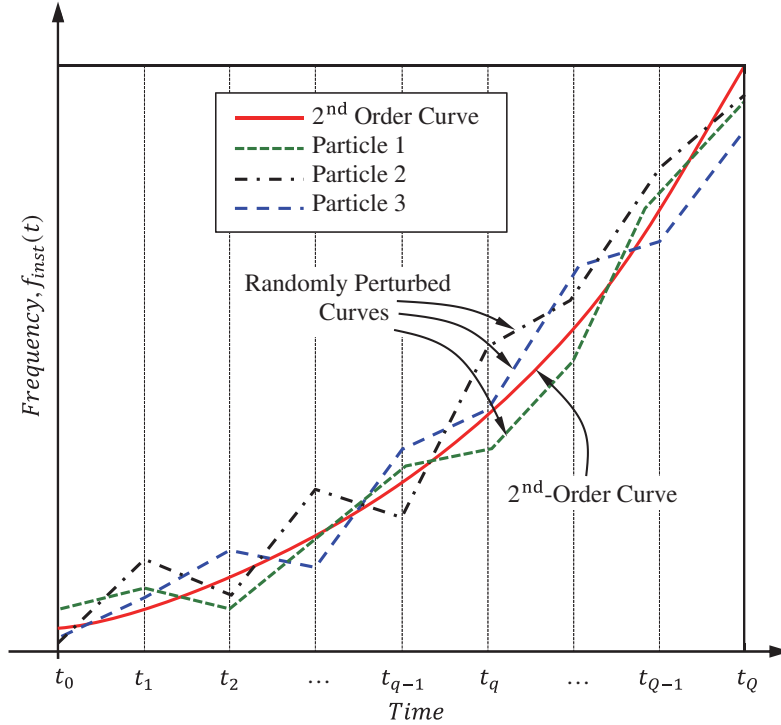
Figure 6. Initialization of the time-frequency curve corresponding to the different particles of the swarm as 2nd-order curve with random perturbations.

middle of the SAR pulse or by applying a simple optimization process. Small random perturbations are then added to each slope $s_q^{(\nu,0)}$ to get the initial positions of the swarm particles different from each other.

$$S_q^{(\nu,0)} = S_q + r_\nu \tag{21}$$

Unless the random perturbations described by (2) are applied, all the particles of the swarm will have the same position, which causes the iterations of the PSO to diverge. However, during the application of the random perturbations, the linear segments of the PWL time-frequency curve should be continuous, i.e., the start point of the qth linear segment should be coincident with the end point of the $(q-1)^{\text{th}}$ linear segment. For initialization, the local best position of each particle, $\mathbf{y}_\nu^{(0)}$, is set equal to the particle position, $\mathbf{x}_\nu^{(0)}$. Also, the velocity vector of each particle is initialized as zero vector; $\mathbf{v}_\nu^{(0)} = \mathbf{0}$.

4.2.2.2 Progressive Iterations of the PSO Algorithm

For each particle in the swarm, the position that gives the minimum cost over the past iterations of the PSO algorithm is recorded as the local best position, $\mathbf{y}_\nu^{(\tau)}$ of this particle. The global best position, $\mathbf{g}^{(\tau)}$, is the particle position among all the particles of the swarm that gives the minimum cost over the past iterations. In each iteration, the velocity, $\mathbf{v}_\nu$, and position, $\mathbf{x}_\nu$, of each particle are evaluated by expressions (18) and (19), respectively.

4.3. Calculation of the Maximum PSLR, PCR, and Range Resolution

The processed echo signal at the receiver output has its time dependence as sketched in Figure 7. The pulse is normalized and plotted using decibel scale. The duration of the processed echo can be calculated as the width of the main lobe (the time between the first two nulls) as shown in Figure 7. The PSLR is
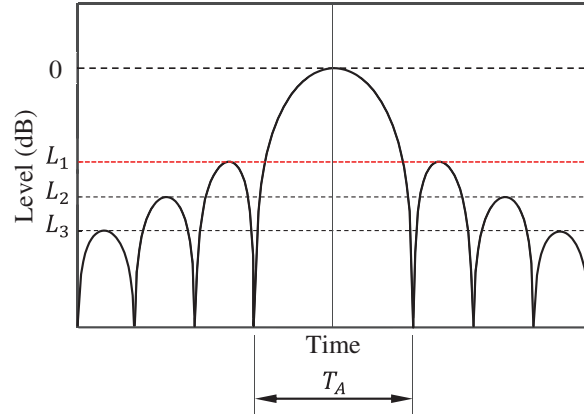
Figure 7. Sketch of the time-dependence of the normalized pulse, $p(t)$ at the output of the MF of the proposed SAR system receiver.

equal to the maximum level of lobes excluding the main lobe. As shown in Figure 7, it is usually found that the second lobe (the first side lobe) has the maximum level among all the side lobes. In this case, the maximum PSLR is L_1 (dB), and the compressed pulse width is T_A. The PCR is defined as follows.

$$\text{PCR} = \frac{T}{T_A} \tag{22}$$

It should be noted that the calculation of the PSLR in the following investigations depends on the determination of the maximum side lobe level among all the side lobes, which is not necessarily the second lobe level. The objective of the design of the proposed SDR-based receiver of the SAR system is to minimize the PSLR and to satisfy a desired (predefined) PCR.

The achieved range resolution, ρ_r, resulting from the application of the proposed compression scheme can be calculated as follows.

$$\rho_r = \frac{cT_A}{2\sin\theta_L} \tag{23}$$

where θ_L is the look angle of the SAR system that operates in the strip-mapping mode.

5. RESULTS AND DISCUSSIONS

In the present section, some numerical examples are presented and discussed to investigate the signal processing scheme proposed for enhancing the detection performance and improving the resolution of the land imaging SAR systems. However, before presenting these examples, the performance of the conventional NLFM pulse chirping method based on quadratic time dependence of the instantaneous frequency is presented and discussed to be used as a reference for evaluating the performance of the proposed method. It should be noted that the proposed pulse compression scheme is applied to improve the resolution in the range direction for a side-looking SAR system that operates in the strip-mapping mode. In the following numerical investigations, it is assumed that the SAR system operates with a look angle $\theta_L = 45°$.

5.1. Conventional Second-Order NLFM for SAR Pulse Chirping

The NLFM using second-order (quadratic) frequency-time dependence of the instantaneous frequency is a well-known method for enhancing the detection performance and improving the resolution of the land-imaging SAR systems. Before chirping, a rectangular pulse of duration $T = 50\,\text{ns}$ is presented in Figure 8(a). The instantaneous frequency increases as a quadratic function of the time as given by (3) with $A = 3.395 \times 10^{23}\,\text{s}^{-3}$. The resulting time-frequency curve is presented in Figure 8(b). In this case, the chirped pulse has the time waveform, $s(t)$, presented in Figure 9(a) and the spectrum, $S(f)$, presented in Figure 9(b).
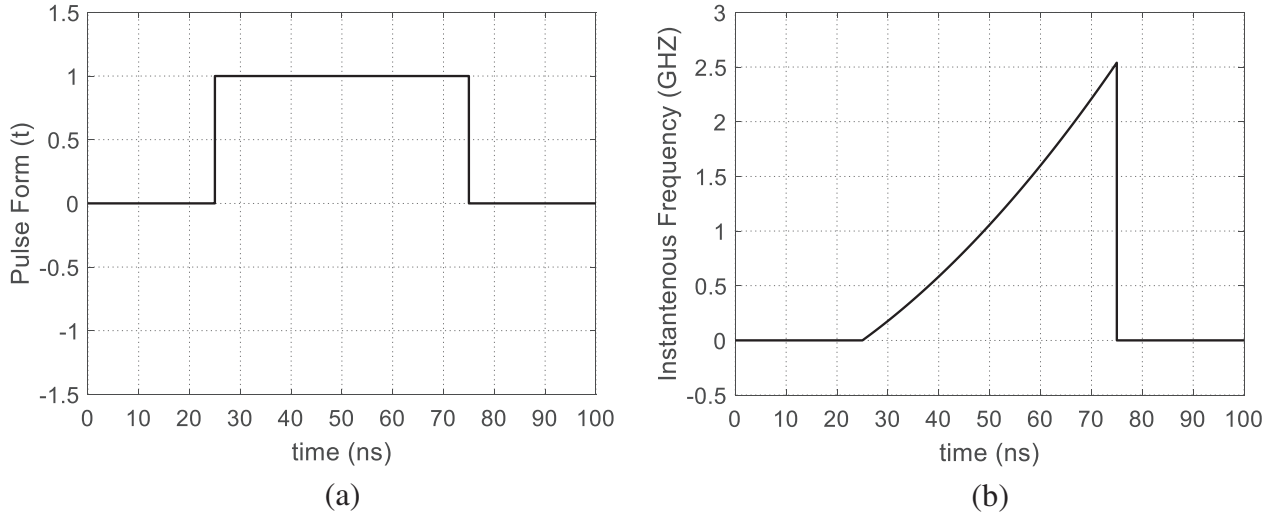
Figure 8. (a) The rectangular pulse before being chirped. (b) Second-order time-frequency curve as described by expression (3) with $A = 3.395 \times 10^{23}\,\text{s}^{-3}$.
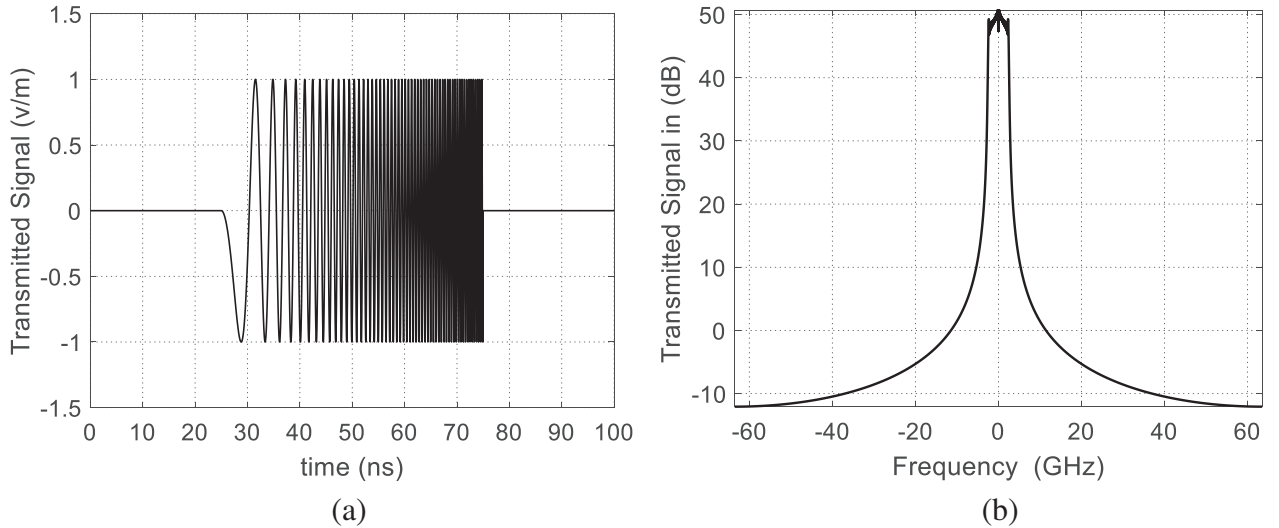

Figure 9. The chirped pulse using second-order time-frequency curve for NLFM: (a) Time-waveform of the chirped pulse, $s(t)$. (b) Spectrum of the chirped SAR pulse $S(f)$.

The received echo pulse, $r(t)$, which is backscattered from the radar target due to the incidence of the chirped pulse, $s(t)$, is processed in the SDR-based receiver by the MF as described in Section 3. The MF processing of $r(t)$ results in the processed SAR echo, $p(t)$, whose time-waveform is shown in Figure 10. It is shown that the maximum PSLR of $p(t)$ is about $-18\,\text{dB}$. Also, it is clear that the time duration of the main lobe (time interval between the first two nulls) is very small relative to the duration T of the transmitted SAR pulse, $s(t)$. The width of the main lobe of $p(t)$ is $0.44\,\text{ns}$. According to (21), the resulting PCR is 115, which is obtained by dividing the duration T of the transmitted pulse presented in Figure 8(a) by the duration, T_A, of the main lobe of $p(t)$. Thus, the frequency chirping using the conventional second-order NLFM (quadratic time-dependence of the instantaneous frequency) results in very high PCR, but the resulting PSLR is about $-18\,\text{dB}$. It may be recommended, in many applications, to further reduce the PSLR for more precise SAR imaging with higher detection performance. Therefore, the optimized PWL time-frequency curve proposed in the present work is
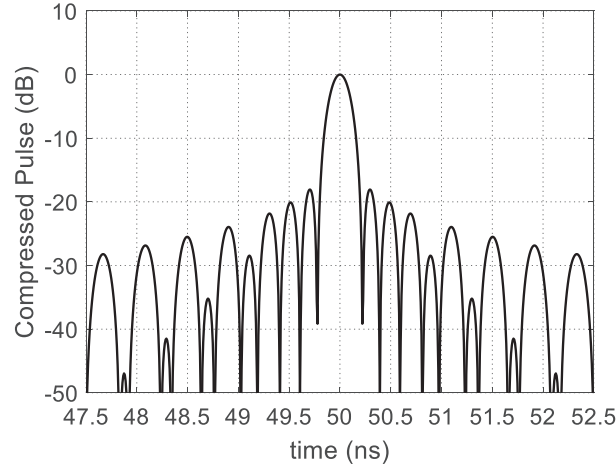
Figure 10. Time-waveform of the processed echo pulse at the output of the MF due to the application of SAR pulse chirping by the conventional second-order dependence of the instantaneous frequency on the time. The resulting PSLR is 18 dB and the PCR is 115.

suggested to enhance the SAR system detection performance and resolution as demonstrated by the examples presented in the following subsections.

5.2. Performance Assessment of the Proposed Pulse Compression Scheme

Some numerical examples are presented to investigate the performance of the proposed signal processing scheme using the optimized PWL time-frequency curve for pulse chirping as described in Section 4. The PSO algorithm runs to achieve the desired value of the PCR with the minimum PSLR. Owing to its computational efficiency, the proposed PSO algorithm takes a few iterations to arrive at the optimum value of the PSLR and desired PCR. The application of the PSO algorithm results in constructing the PWL segmented curve for the variation of the instantaneous frequency with the time, thereby reducing the PSLR from its initial value $(-18\,\mathrm{dB})$ that has been obtained using the conventional second-order frequency chirping method demonstrated in Subsections 2.1 and 5.1 to a much better value.

The number of linear segments, Q, used to construct the time-frequency curve can be used as a parameter to get varying values of the PCR and the corresponding PSLR. It will be shown from the present simulation results that increasing Q has the positive effect of decreasing the PSLR in one hand and the negative effect of decreasing the PCR in the other hand. A compromise should be made to select the value of Q that achieves the decided optimization goals of the SAR pulse compression using the proposed technique. For example, the maximum PCR can be achieved using $Q = 1$ (i.e., linear time-frequency curve) and is almost 127, which is the PCR obtained by the conventional LFM method. In this case, the PSO goals are to minimize the PSLR keeping the PCR as close as possible to 127. As the time-frequency curve has only one segment with a slope s_1, there is no control parameters to be used by the PSO to get performance better than that obtained by the conventional LFM pulse compression technique. The time-frequency curve shown in Figure 11(a) is obtaine,d and the resulting time waveform of the processed echo signal, $p(t)$, at the MF output is presented in Figure 11(b). In this case, the achieved PSLR is $-13\,\mathrm{dB}$, and the achieved PCR is 127, which is the well-known performance of the conventional LFM.

In another example, to achieve a PCR of 120, the number of the linear segments is set to $Q = 2$. In this case, the PSO goals are to minimize the PSLR keeping the PCR as close as possible to 120. As the time-frequency curve has only two segments, the control parameters of the PSO, in this case, are s_1 and s_2, which are the slopes of the two linear segments of the time-frequency curve. The PSO algorithm produces the time-frequency curve shown in Figure 12(a). The resulting time-waveform of the processed echo signal, $p(t)$, at the MF output is presented in Figure 12(b). In this case, the achieved PSLR is $-19\,\mathrm{dB}$, and the achieved PCR is 119.
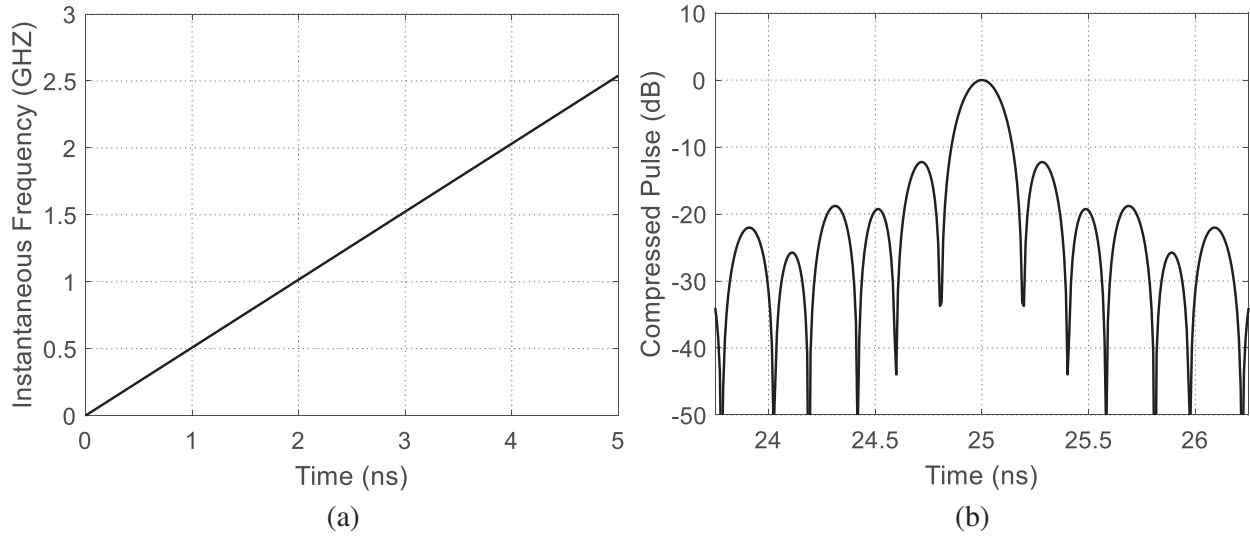
Figure 11. The instantaneous frequency curve of one segment, $Q= 1$ (equivalent to LFM) leads to a processed echo signal with PSLR of -13 dB and PCR of 127. (a) The time-frequency curve. (b) The processed echo signal, $p(t)$ at the MF output.
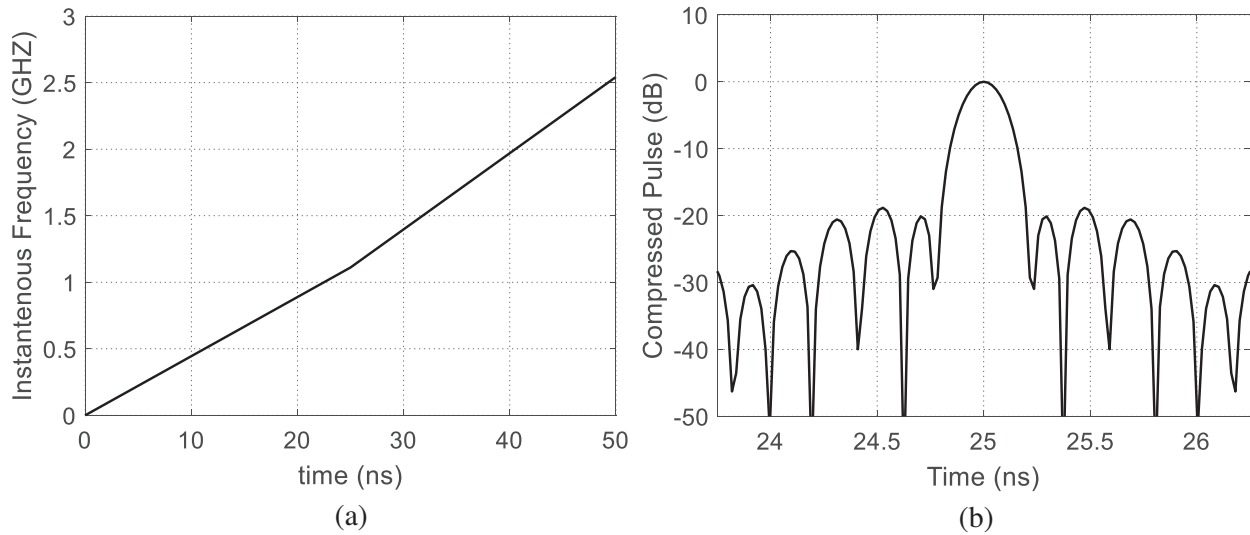

Figure 12. Optimization of the time-frequency curve using only two linear segments ($Q= 2$) to achieve PSLR of -19 dB and PCR of 119. (a) The optimized time-frequency curve. (b) The processed echo signal, $p(t)$ at the MF output.

In a third example, the optimization goals are to minimize the PSLR and to obtain a PCR of 75. For this value of the PCR, it is appropriate to set $Q = 10$. In this case, the PSO algorithm produces the time-frequency curve, $f_i(t)$, shown in Figure 13(a). The resulting time waveform of the processed echo signal, $p(t)$, at the MF output is shown in Figure 13(b). The achieved PSLR is -28 dB, and the achieved PCR is 80.

For further decrease of the PSLR, a fourth example is demonstrated in Figure 14, where the optimization goals are to minimize the PSLR and to obtain a PCR of 55. In this case, it may be appropriate to set $Q = 30$, where the PSO algorithm produces the time-frequency curve, $f_i(t)$, shown in Figure 14(a). The resulting time waveform of the processed echo signal, $p(t)$, at the MF output is shown in Figure 14(b). In this case, the achieved PSLR is -34 dB, and the PCR is 50.
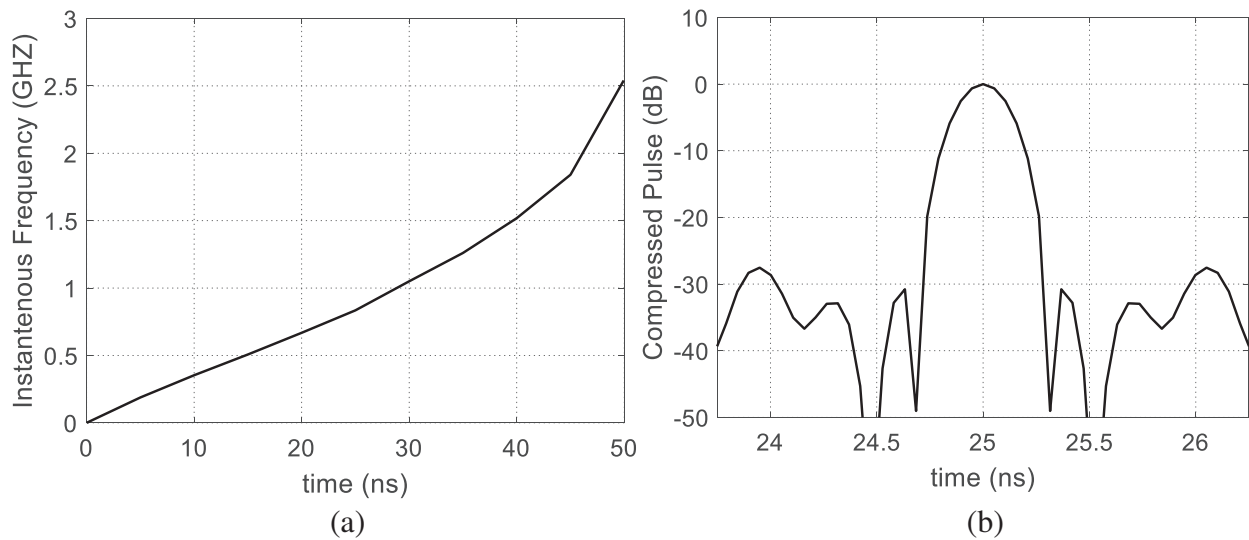
Figure 13. Optimization of the time-frequency curve using $Q = 10$ linear segments to achieve a processed echo signal with PSLR of $-28\,$dB and PCR of 80. (a) The optimized time-frequency curve, $f_i(t)$. (b) The processed echo signal, $p(t)$, at the MF output.
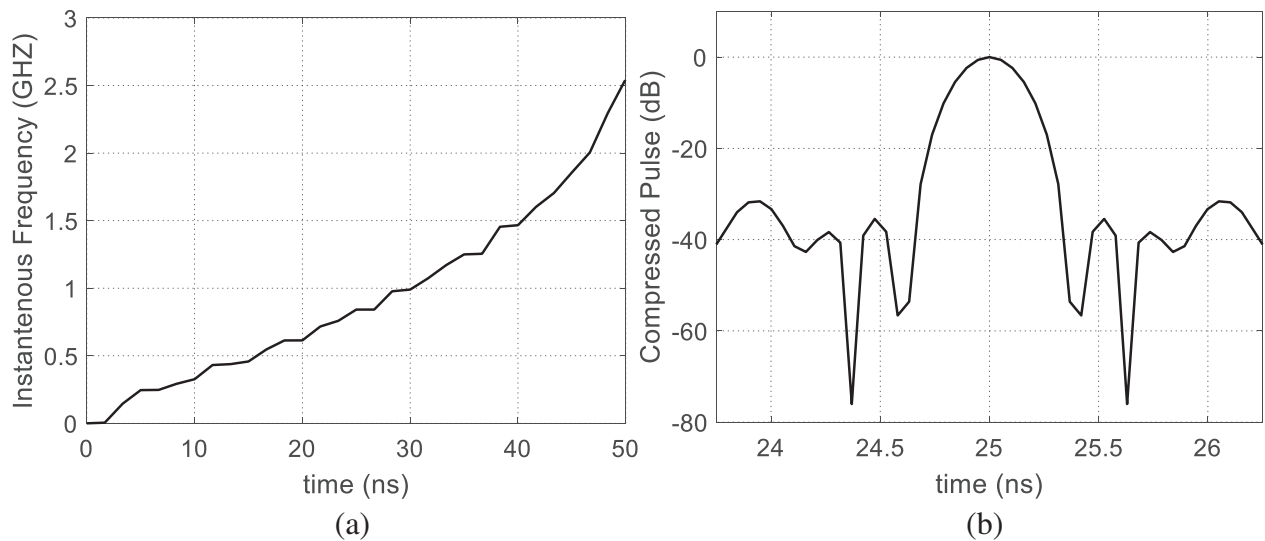

Figure 14. Optimization of the time-frequency curve using $Q = 30$ linear segments to achieve a processed echo signal with PSLR of $-34\,$dB and PCR of 50. (a) The optimized time-frequency curve, $f_i(t)$. (b) The processed echo signal, $p(t)$, at the output of the MF.

5.3. Computational Efficiency of the PSO Algorithm

In addition to the simplicity of the PSO algorithm developed in the present work to optimize the radar pulse compression using the piecewise linearly segmented time-frequency curve proposed as a scheme for NLFM, it is characterized by its computational efficiency and fast convergence. It takes a few iterations to perform the required optimization goals such that the cost function decays to less than 20% of its initial (at the beginning of the algorithm) just after the first iteration. A little decay of the cost function is observed in the second iteration and settled down to each steady state value just after the third iteration. For example, the decay curves of the cost function during the optimization process for the three cases presented in Subsection 5.2 for $Q = 2, 10, 30$ are presented in Figures 15(a), (b), (c),
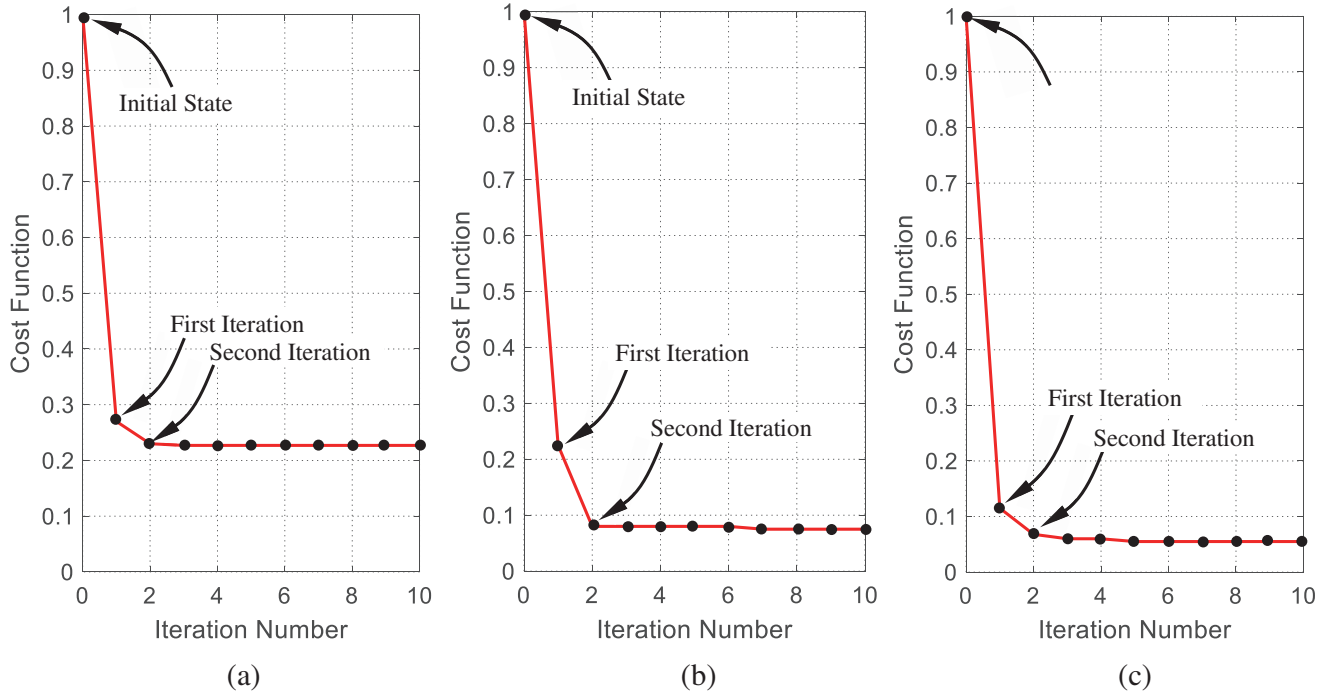
Figure 15. Fast decay of the cost function with the running iterations of the PSO algorithm for the SAR pulse compression cases whose results are presented in Figures 12, 13, and 14. (a) $Q = 2$. (b) $Q = 10$. (c) $Q = 30$.

respectively. Such fast decay rate gives the PSO algorithm advantage over the other multi-objective evolutionary optimization techniques that can be used for achieving the goals of reducing the PSLR and realizing a specific PCR.

5.4. Relation between the Achieved PCR, PSLR and the Number of Linear Segments

From the presentation of the previous examples, it is shown that the PCR decreases with increasing the number of linear segments, Q of the PWL time-frequency curve. On the other hand, the maximum PSLR is improved (decreases) with increasing Q. The relations governing the dependence of the maximum PSLR and the corresponding PCR on the number of linear segments, Q, of the PWL time-frequency curve are presented in Figure 16(a). It may be useful to plot the relation between the achievable PSLR as a function of the (corresponding) PCR. This relation is presented in Figure 16(b). It is noticed that increasing Q leads to decreasing both the PSLR and the PCR. Also, it is clear that both the PSLR and PCR reach their saturation values where Q is increased beyond 35.

5.5. Effect of the SAR Pulse Width on the Performance of the Pulse Compression Scheme

In the previous examples, the SAR pulse duration is set as $T = 50$ ns. The effect of increasing the SAR pulse duration (the time duration of frequency chirping) is depicted in Figure 17. Increasing the SAR pulse width to 180 ns results in the optimized time-frequency curve presented in Figure 17(a) and the time-waveform of the processed echo presented in Figure 17(b). The resulting PSLR is -45.6 dB, which is a considerable improvement regarding the PSLR achieved in the previous examples. On the other hand, the resulting range resolution is $\rho_r = 1.4$ m.
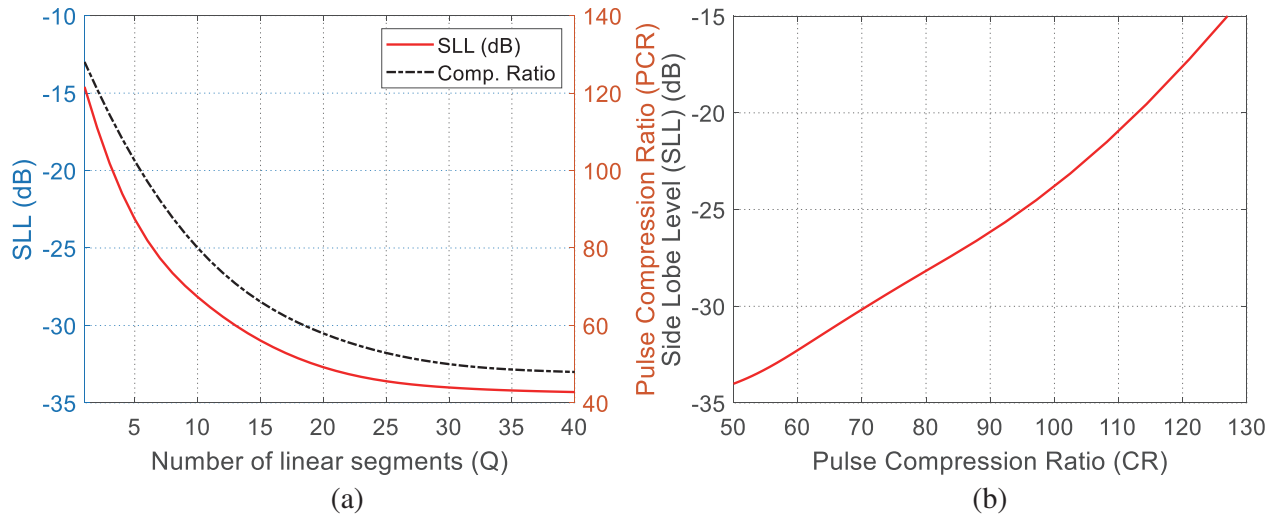
Figure 16. Variation of the PSLR and PCR after applying the PSO. (a) Dependencies of the PSLR and PCR on the number of linear segments of the frequency-time curve. (b) Relation between the achievable PSLR and the corresponding PCR.
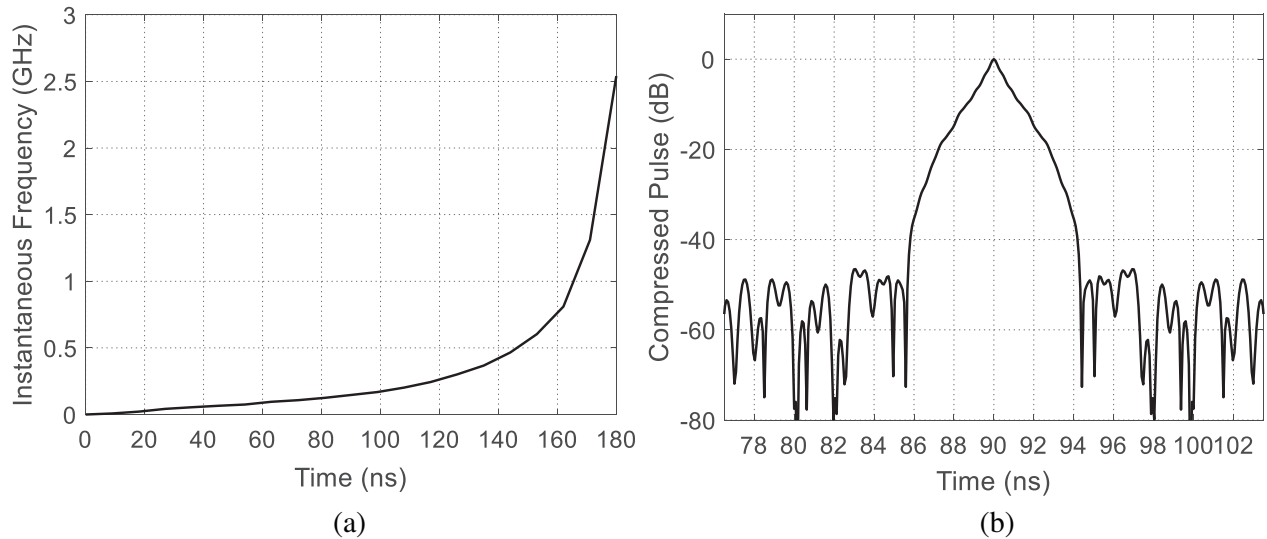

Figure 17. Optimization of the time-frequency curve using $Q = 20$ linear segments to achieve a processed echo signal with PSLR of -45.6 dB, PCR of 3 and range resolution $\rho_r = 1.4$ m. The SAR pulse width is $T = 180$ ns. The chirp bandwidth is $B = 2.54$ GHz. (a) The optimized time-frequency curve, $f_i(t)$. (b) The processed echo signal, $p(t)$, at the output of the MF.

5.6. Effect of the Chirp Bandwidth on the Performance of the Pulse Compression Scheme

In the example discussed in Subsection 5.5, the SAR pulse duration is set as $T = 180$ ns, and the chirp bandwidth (the difference between the end and start frequencies over the SAR pulse duration) is set as $B = 2.54$ GHz. The effect of decreasing the chirp bandwidth is depicted in Figure 18. Decreasing the chirp bandwidth to $B = 2.29$ GHz results in the optimized time-frequency curve presented in Figure 18(a) and the time-waveform of the processed echo presented in Figure 18(b). The resulting PSLR is -21 dB, and the resulting range resolution is $\rho_r = 0.2$ m.
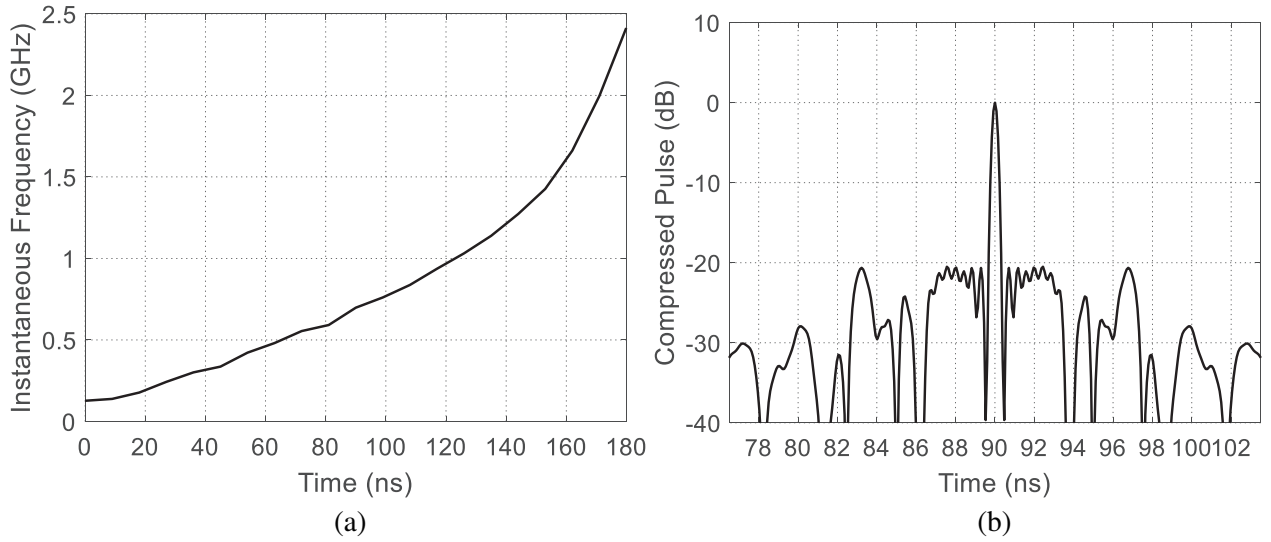
Figure 18. Optimization of the time-frequency curve using $Q = 20$ linear segments to achieve a processed echo signal with PSLR of $-21\,\text{dB}$, PCR of 19 and range resolution $\rho_r = 0.2\,\text{m}$. The SAR pulse width is $T = 180\,\text{ns}$. The chirp bandwidth is $B = 2.29\,\text{GHz}$. (a) The optimized time-frequency curve, $f_i(t)$. (b) The processed echo signal, $p(t)$, at the output of the MF.

5.7. Comparative Performance Summary

The best value of the PSLR of the processed SAR echo at the receiver output achieved by the proposed pulse compression scheme and the resulting range resolution are listed in Table 1. The proposed scheme gives better achieved PSLRs than those achieved PSLRs by other pulse compression schemes proposed in some recent publications as demonstrated in Table 1. However, the SAR signal processing scheme proposed in the present work can produce a processed echo signal with lower PSLR than those achieved in the listed published work depending on the desired PCR. Nevertheless, the PSLR achieved by the signal processing scheme proposed in the present work is variable and depends on the number of linear segments, Q, used to construct the PWL time-frequency curve. Unlike the other pulse compression techniques presented in the recently published research work, the optimization method proposed in the present work allows the selection of the PCR for which the PSLR can then be minimized. It is noticed that increasing the number of linear segments, Q, up to a saturation limit, leads to lower value of the achievable PSLR on the account of the achievable PCR.

It should be noted that the methods listed in Table 1 are briefly described in the "Introduction"

Table 1. Comparisons between the PSLR and the corresponding range resolution achieved in the present work and those achieved by other SAR pulse compression schemes available in some recent publications.

Pulse Compression Scheme	PSLR	Resolution
[16] Starring spotlight mode with NLFM	$-22\,\text{dB}$	$0.414\,\text{m}$
[17] Distinctive piecewise NLFM modulation	$-27\,\text{dB}$	$3.606\,\text{m}$
[18] OFDM based on Piecewise NLFM	$-28\,\text{dB}$	NA
[19] Piecewise NLFM	$-36.6\,\text{dB}$	NA
[20] Optimization using Lagrangian Method	$-38\,\text{dB}$	NA
[21] NLFM based on the ALGA and PWL functions	$-40\,\text{dB}$	$6.364\,\text{m}$
[22] NLFM optimized by genetic algorithm	$-40.6\,\text{dB}$	NA
Present Work (NLFM optimized by PSO)	$-45.6\,\text{dB}$	$1.4\,\text{m}$

section of the present paper. Also, it is noticed that the PSLR is improved whenever combined techniques like those presented in [19–22] are applied to obtain PSLRs of $-36.6\,\mathrm{dB}$, $-38\,\mathrm{dB}$, $-40\,\mathrm{dB}$, and $-40.6\,\mathrm{dB}$, respectively. The lowest SLL obtained using the pulse compression method proposed in the present work is $-45.6\,\mathrm{dB}$, and the corresponding range resolution is $1.4\,\mathrm{m}$ (Section 5.5).

6. CONCLUSION

A novel technique has been proposed to reduce the PSLR and compress the SAR pulse. The proposed technique is based on formulating the time-frequency dependence as arbitrarily shaped PWL curve. The PSO method is used to optimize the shape of the time-frequency curve to achieve the dual-objective of minimizing the PSLR of the SAR pulse at the output of the SAR receiver and to realize a specific desired PCR. The slopes of the linear segments of the time-frequency curve are the control parameters that determine the position of each particle in the swarm. A PSLR of $-45.6\,\mathrm{dB}$ and range resolution of $1.4\,\mathrm{m}$ have been achieved using the proposed optimization method. The developed PSO algorithm has been shown to be computationally efficient, and its iterations are fastly convergent such that a few iterations are enough to arrive at the steady state of the cost function. The proposed SAR pulse compression technique has been implemented in the SDR-based transceiver of the SAR system.

REFERENCES

1. Zhou, Y., W. Wang, Z. Chen, Q. Zhao, H. Zhang, Y. Deng, and R. Wang, "High-resolution and wide-swath SAR imaging mode using frequency diverse planar array," *IEEE Geoscience and Remote Sensing Letters*, Vol. 18, No. 2, 321–325, 2021.
2. Wei, S., X. Zeng, Q. Qu, M. Wang, H. Su, and J. Shi, "HRSID: A high-resolution sar images dataset for ship detection and instance segmentation," *IEEE Access*, Vol. 8, 120234–120254, 2020.
3. Soliman, S. A. M., K. F. A. Hussein, and A. E. H. A. Ammar, "Electromagnetic simulation for estimation of forest vertical structure using PolSAR data," *Progress In Electromagnetics Research*, Vol. 90, 129–150, 2021.
4. Soliman, S. A. M., K. F. A. Hussein, and A. E. H. A Ammar, "Electromagnetic resonances of natural grasslands and their effects on radar vegetation index," *Progress In Electromagnetics Research B*, Vol. 86, 19–38, 2020.
5. Kumar, A. and M. Nidhi, "Radar pulse compression technique for linear frequency modulated pulses," *International Journal of Engineering and Technical Research (IJETR)*, Vol. 3, No. 8, 2454–4698, ISSN: 2321-0869, August 2015.
6. Skolnik, M. I., *Radar Handbook*, 3rd Edition, McGraw-Hill, New York, 2008.
7. Likhith Reddy, D. and S. V. Subba Rao, "A novel design of matched filter for digital receivers," *International Journal of Recent Technology and Engineering (IJRTE)*, Vol. 8, No. 3, ISSN: 2277-3878, September 2019.
8. Chan, Y. K., B.-K. Chung, and H.-T. Chuah, "Transmitter and receiver design of an experimental airborne synthetic aperture radar sensor," *Progress In Electromagnetics Research*, Vol. 49, 203–218, 2004.
9. Grabowski, A., "SDR-based LFM signal generator for radar/SAR systems," *2016 17th International Radar Symposium (IRS)*, 1–3, IEEE, 2016.
10. Vizitiu, I. C., "Some aspects of sidelobe reduction in pulse compression radars using NLFM signal processing," *Progress In Electromagnetics Research C*, Vol. 47, 119–129, 2014.
11. Galushko, V. G., "On application of taper windows for sidelobe suppression in LFM pulse compression," *Progress In Electromagnetics Research C*, Vol. 107, 259–271, 2021.
12. Abd-Elfattah, A. G. A., K. F. A. Hussein, A. E. Farahat, and M. A. Kotb, "Electromagnetic simulation for robust recognition algorithm of radar target by homing missiles," *Progress In Electromagnetics Research B*, Vol. 97, 37–54, 2022.

13. Hussein, K. F. A., A. O. Helmy, and A. S. Mohra, "Radar pulse compression with optimized weighting window for SAR receivers," *Wireless Personal Communications*, Vol. 126, No. 1, 871–893, Sep. 2022.

14. Ackroyd, M. H. and F. Ghani, "Optimum mismatched filters for sidelobe suppression," *IEEE Transactions on Aerospace and Electronic Systems, AES-9*, Vol. 2, 214–218, 1973.

15. DeGraaf, S. R., "Sidelobe reduction via adaptive FIR filtering in SAR imagery," *IEEE Transactions on Image Processing*, Vol. 3, No. 3, 292–301, 1994.

16. Xu, W., L. Zhang, C. Fang, P. Huang, W. Tan, and Y. Qi, "Staring spotlight SAR with nonlinear frequency modulation signal and azimuth non-uniform sampling for low sidelobe imaging," *Sensors*, Vol. 21, 6487, 2021, https://doi.org/10.3390/ s21196487.

17. Zhao, Y., X. Lu, M. Ritchie, W. Su, and H. Gu, "Suppression of sidelobes in MIMO radar with distinctive piecewise non-linear frequency modulation sub-carrier," *International Journal of Remote Sensing*, DOI: 10.1080/01431161.2019.1641644, 2019.

18. Zhao, Y., X. Lu, J. Yang, W. Su, and H. Gu, "OFDM wavefroms designed with piecewise nonlinear frequency modulation pulse for MIMO radar," *International Journal of Remote Sensing*, DOI: 10.1080/01431161.2018.1490978, 2018.

19. Gao, C., K. C. Teh, and A. Liu, "Piecewise nonlinear frequency modulation waveform for MIMO radar," *IEEE Journal of Selected Topics in Signal Processing*, DOI 10.1109/JSTSP.2016.2616108, 2016.

20. Roohollah, G. and M. A. Sebt, "Sidelobe level reduction in ACF of NLFM waveform," *IET Radar, Sonar & Navigation*, Vol. 13, No. 1, 74–80, 2019.

21. Jin, G., Y. Deng, Member, R. Wang, W. Wang, P. Wang, Y. Long, Z. Zhang, and Y. Zhang, "An advanced nonlinear frequency modulation waveform for radar imaging with low sidelobe," *IEEE Transactions on Geoscience and Remote Sensing*, Vol. 57, No. 8, August 2019.

22. Wei, T., W. Wang, Y. Zhang, and R. Wang, "A novel nonlinear frequency modulation waveform with low sidelobes applied to synthetic aperture radar," *IEEE Geoscience and Remote Sensing Letters*, Vol. 19, 1–5, 2022.

23. Wang, D., D. Tan, and L. Liu, "Particle swarm optimization algorithm: An overview," *Springer*, Verlag Berlin Heidelberg, Published online, January 17, 2017.